Chemical Methodologies

journal homepage: http://chemmethod.com

Original Research article

Electrochemical and Simulation Analysis of Salen as a Corrosion Inhibitor

Homa Shafiekhani[a], Fatemeh Mostaghni[a] *, Kolsoum Ejraei[b]

[a] Payam Noor University, Department of Chemistry, Tehran, Iran
[b] Islamic Azad University Lamerd Branch, Lamerd, Iran

ARTICLE INFORMATION

Received: 09 October 2017
Received in revised: 02 February 2018
Accepted: 18 February 2018
Available online: 01 March 2018

DOI:
10.22631/chemm.2018.112578.1030

KEYWORDS

Acid corrosion
Electrochemical techniques
Density functional theory
Simulation analysis

ABSTRACT

The potentiodynamic polarization curves, quantum chemical calculation and molecular dynamics simulation methods are used to study the inhibition effects of Salen ligand regarding the corrosion of carbon steel (A105) in salty and acidic solutions of 3.5% NaCl and 1.0 M HCl respectively. The results show that the values of inhibition efficiency in 3.5% NaCl and 1.0 M HCl solutions are higher than 96% and 95% respectively at 25 °C. For both solutions, the adsorption of the inhibitor on steel surface corresponds the Langmuir adsorption isotherm, and the nature of adsorption is mainly chemical. All the results show that Salen is a good corrosion inhibitor for protection of steel in both Salty and acidic medium.

Corresponding author, email: mostaghnif@yahoo.com
Payam Noor University, Iran, Chemistry Department,Tel: 0098-71-44354061; Fax: 0098-71- 44354071

Graphical Abstract

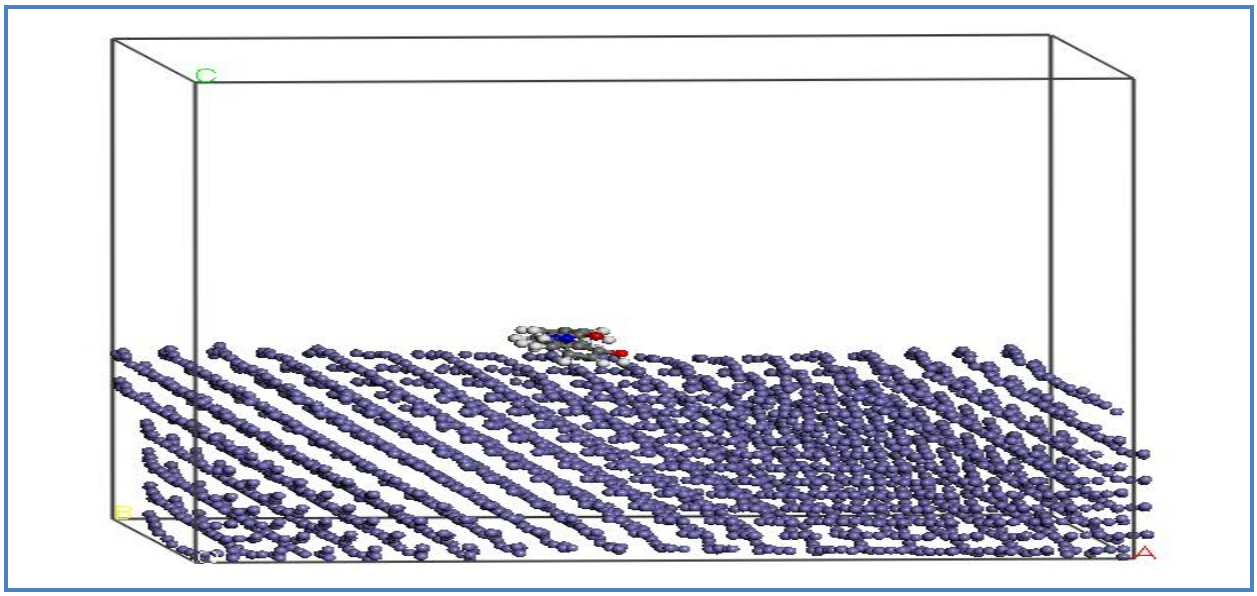

Introduction

Vast literature reports show that corrosion is a serious problem especially for metals and alloys used in industries and that it can economically and drastically affect the productivity and life time of an industry. Iron and carbon steel are two major metals widely used in all kinds of industries and engineering applications. Therefore, the corrosion inhibitions of iron and carbon steel in salty and acidic medium are the major concern of researchers for both industrial and academic purposes [1]. There are several methods for controlling the corrosion processes such as: cathodic protection, anodic protection, coating and alloying methods. However, the application of chemical inhibitors which is a very popular and economically advantageous method to control the corrosion process can finally protect the industries [2-9].

Acid corrosion inhibitors are mostly organic compounds with polar functions containing S, O or N atoms in the molecule, in addition, heterocyclic groups and π-electrons are also common [10-14]. These inhibitors can form a protective film on the surface of the metal through chemisorption or physisorption processes. In this regard, Salen-type Schiff base ligands or their derivatives have a great importance in coordination chemistry.

Some researches show that the inhibition efficiency of Schiff base is much higher than that of corresponding amines and aldehydes [15]. The efficiency of salen-type Schiff base molecules and their derivatives are associated with the presence of hetero atoms of nitrogen, oxygen and π-electrons in the molecule and this property makes them to be very effective inhibitors. In fact, these properties induce high ligating power in Salen ligands and, due to good absorption phenomena, can

produce large molecular surface area and complete covering of metal surfaces [16-17]. Evaluation and prediction of inhibition performance of Salen-type ligands primarily have been conducted experimentally by using techniques such as weight loss assessment, electrochemical potentiodynamic, polarization resistance, and AC impedance (EIS) [18-23].

A powerful tool such as quantum chemical calculation has been used to find out a correlation between molecular structure and inhibition efficiency [24-30]. However, the molecular dynamics (MD) simulations have been used to study the interaction between the adsorbed molecules of inhibitor and the corroded metal surface [31,32].

In this paper, tetradentate N,N'-bis(salicylaldehyde) ethylenediimine (Salen) is used as an effective corrosion inhibitor. The inhibitory effect of salen-H2 on the corrosion process of steel (A105) in NaCl 3.5% and 1.0 M HCl solutions was studied using potentiodynamic polarization curves method, and, also, the adsorption isotherm of inhibitor on steel surface was obtained.

In addition, density functional theory (DFT) calculations were performed for the title compounds. The energy of the highest occupied molecular orbital (E_{HOMO}), the energy of the lowest unoccupied molecular orbital (E_{LUMO}), the energy gap E_{HOMO}- E_{LUMO} (ΔE), dipole moment (μ), elctronegativity (χ) and global hardness (η) of the title compounds were calculated at the DFT-B3LYP level of theory using the 6-31G$^+$ basis set.

Morevere, we used MD simulations for investigation of the adsorption of inhibitor molecule on Fe (001) surface. The main scope of this study was to obtain general information on the adsorption and inhibitory effect of Salen on carbon steel in NaCl and HCl solutions.

Experimental

Material

All chemicals were analytical grade and used without purification. The steel used in this study was one type of a carbon steel (A105) with a chemical composition (in wt%) of 0.35% C, 0.6-1.05% Mn, 0.035% P, 0.04% S, 0. 1-0.35% Si, 0.3 % Cr, 0.08 % V, 0.4 % Ni, 0.009% Mo, 0.4 % Cu and balance Fe . The molar solution HCl was prepared by dilution of analytical grade 37% HCl with distilled water. The concentration range of the used inhibitors was 0.002–0.2 mM.

Synthesis of Salen

The amount of 4.0 mmol of 2-hydroxybenzaldehyde in ethanol (50 ml) was added dropwise to ethanolic solution(10 ml) of 2.0 mmol ethylenediamine. This mixture was refluxed for 2 h. Afterwards the mixture was cooled to room temperature, then cooled for 24 h at 5 ^{o}C. The yellow solid was filtered off and recrystallized from ethanol [33]. Yield: 92.5%. m.p.: 125 ^{o}C .

Selected IR bands (KBr) (ν_{max}/ cm^{-1}): 3450 (OH); 1635s (C=N); 1576m (C=C); 1371m (C-N); 1283m (C-O); UV–Vis (DMSO): λmax=410 (nm).

Potentiodynamic Polarization Studies

Electrochemical measurements were carried out using a μAutolabIII (PGSTAT30) potentiostate galvanostate and controlled by NOVA1.5 software. The electrochemical cell consisted of a three electrode setup in which a platinum electrode was used as counter electrode, the reference electrode was a saturated calomel electrode (SCE), and the working electrode was carbon steel (A105).

The test surface area of W.E was 1X1 cm^2, and was abraded with different grades of emery paper, degreased in acetone, rinsed with double distilled water, and finally dried at room temperature before use. Before measurements of polarization curves, the working electrode was immersed in test solution for 30 minutes to an establish steady state open circuit potential (E_{ocp}). The polarization curves were recorded in the potential range from -250 to 250 mV vs. OCP with an scan rate of 2 mV/s.

Quantum mechanical calculation

All geometry optimizations and quantum chemical calculations were carried out with the Gaussian program 09 as basic program and Gaussian Viewer as graphical medium. The calculations of DFT were carried out using the three B3LYP functionals. The usual 6-31G basis set was employed in the DFT calculations [34].

MD simulations

Molecular dynamic simulations (MD) of the interaction between inhibitor molecules and the metal surfaces was carried out using Materials Studio 6.0 (from Accelrys Inc) [35,36].

Fe (001) plane was firstly cleaved from pure Fe crystal and the surface was then optimized to the energy minimum. The basic cell was replicated to obtain a super cell of approximately (18X18X18) with periodic boundary conditions to model a representative part of the interface devoid of any arbitrary boundary effects [37]. Six layers of Fe atoms supplied enough depth. Besides, inhibitor molecules will only be involved in non-bond interactions with Fe atoms in the layers of the surface devoid of increasing the calculation time unreasonably. A vacuum slab of 30 Å thicknesses was kept on the Fe (001) surface. The molecular dynamics simulation was then performed at 298^o K, with a time step of 0.1 fs and simulation time of 0.5 ps. The interaction energy, as well as binding energy between the inhibitor molecules and Fe (001) surface, were calculated using Equation 1 and 2 [38].

$$E_{interaction} = (E_{surface} + E_{inhibitor}) - E_{total} \quad (1)$$

$E_{binding} = - E_{intereaction}$ (2)

where E_{total} is the total energy of the surface and inhibitor, $E_{surface}$ is the energy of the surface without the inhibitor, and $E_{inhibitor}$ is the energy of the inhibitor without the surface. The interaction energy of the inhibitor molecule is the negative value of binding energy.

Results and Discussion

Potentiodynamic polarization Studies

Potentiodynamic polarization curves of Salen in HCl 1.0 M and NaCl 3.5 % solutions with and without addition of different concentrations of inhibitor at 20°C are shown in Figure 1, 2.

Figures 1 and 2 show that both the cathodic and the anodic peaks display a wide region of tafel behaviour.

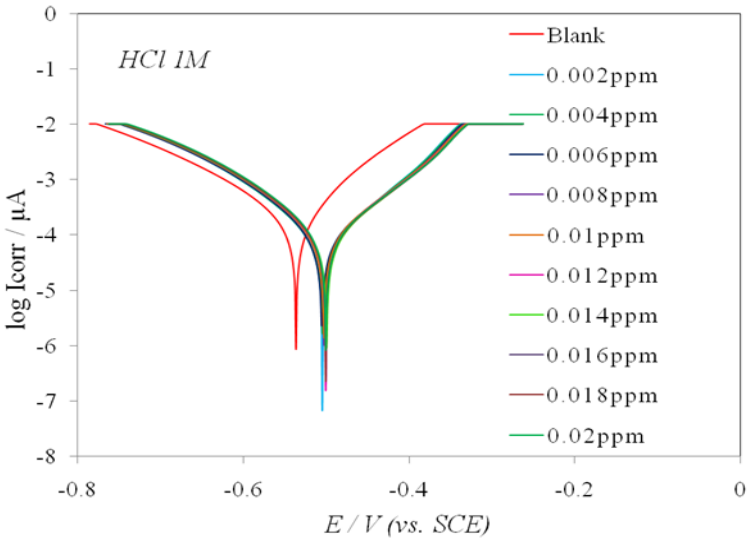

Figure 1. Potentiodynamic polarization curves for Salen in 1.0 M HCl with and without different concentrations of Salen at 20oC (immersion time is 2 h)

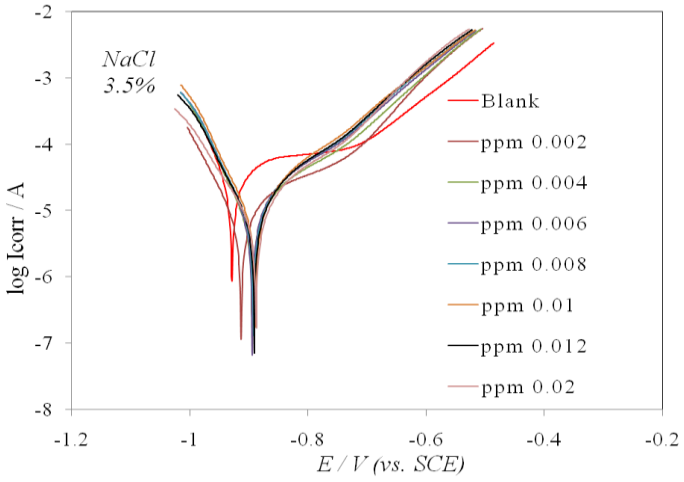

Figure 2. Potentiodynamic polarization curves for Salen in NaCl 3.5% with and without different concentrations of Salen at 20oC (immersion time is 2 h)

The values of associated electrochemical parameters, i.e., corrosion current (i_{corr}), corrosion potential (E_{corr}), anodic Tafel slope (β_a) and cathodic Tafel slope (β_c), in various concentrations of Salen are determined by extrapolation of anodic and cathodic Tafel lines. Inhibition efficiencies (%IE) and degree of coverage (θ) were determined by equations 1 and 2 respectively.:

$$\%IE = \left(1 - \frac{I_{corr}}{I^{o}_{corr}}\right) \times 100 \quad (3)$$

$$\theta = \frac{I^{o}_{corr} - I_{corr}}{I^{o}_{corr}} \quad (4)$$

I^{o}_{corr} and I_{corr} are the corrosion current densities of steel in the presence and absence of inhibitor respectively [39].

The polarization resistance *Rp* is defined as the slope of the linear part of the polarization curve close to the corrosion potential E_{corr} and is also calculated by the following equation [40]:

$$R_p = 2.303 \frac{b_a b_c}{b_a + b_c} \left(\frac{1}{I_{corr}}\right) \quad (5)$$

The corrosion current can be related directly to the corrosion rate (mpy) through the following equation [41]:

$$Corrosion\ Rate\ (mpy) = \frac{0.13 I_{corr}(E.W)}{d} \quad (6)$$

Where E.W. is equivalent weight of the corroding species (g), d is density of the corroding species (g/cm^2)) and I_{corr} is corrosion current density ($\mu A/cm^2$).

However, the NOVA software provides a convenient interface for making Tafel plots, calculating Tafel slopes and corrosion rates. Once the anodic and cathodic Tafel region were selected, Tafel slopes and the corrosion currents were calculated by the NOVA software. All results are summarized in Table 1.

The adsorption of inhibitor can affect the corrosion rate in two ways: (i) geometric blocking effect by decreasing the available reaction area, and (ii) by modifying the activation energy of dissolution of metal (anodic reaction), and the hydrogen evolution (cathodic reaction). It has been reported that the geometric blocking effect is stronger than the energy effect if no remarkably shift in corrosion be observed after addition of the corrosion inhibitor [42], otherwise the energy effect is stronger.

Table 1. Polarization parameters for mild steel in HCl 1M with different concentrations of Salen

Conc	$-E_{corr}$	β_a	β_c	I_{corr}	I.E	R_p	θ	R_{corr}

(ppm)	(mV/SCE)	(mV/dec)	(mV/dec)	(μA/cm²)	(%)	(Ω.cm²)		(mpy)
0	526.10	161.06	103.83	0.337	-	81.38	-	154.1
2×10^{-4}	446.28	178.83	63.74	0.210	37.53	97.03	0.375	96.3
4×10^{-4}	446.80	131.59	99.23	0.167	50.5	147.32	0.505	76.3
6×10^{-4}	451.02	154.18	60.90	0.132	60.91	143.98	0.609	60.2
8×10^{-4}	478.72	119.72	75.08	0.097	71.09	205.75	0.711	44.5
1×10^{-3}	503.84	77.92	89.17	0.074	77.80	241.55	0.778	34.2
1.2×10^{-3}	503.74	40.17	53.40	0.037	88.84	264.78	0.888	17.2
1.4×10^{-3}	502.04	38.79	46.61	0.033	90.18	277.98	0.902	15.1
1.6×10^{-3}	501.51	32.18	36.44	0.027	92.04	276.64	0.920	12.3
1.8×10^{-3}	501.32	25.78	32.66	0.023	93.20	273.00	0.932	10.5
2.0×10^{-2}	499.01	22.20	19.45	0.016	95.02	268.34	0.950	7.70

Table 2. Polarization parameters for mild steel in NaCl 3.5 % with different concentrations of Salen

Conc (ppm)	$-E_{corr}$ (mV/SCE)	β_a (mV/dec)	β_c (mV/dec)	I_{corr} (μA/cm²)	I.E (%)	R_p (Ω.cm²)	θ	R_{corr} (mpy)
0	928.48	107.16	50.01	0.0509	-	407.08	-	23.3
2×10^{-4}	912.94	70.05	176.04	0.0085	83.29	2554.8	0.833	3.9
4×10^{-4}	894.52	46.14	82.46	0.0051	89.83	2479.5	0.898	2.4
6×10^{-4}	895.65	38.36	45.98	0.0036	92.92	2517.1	0.929	1.7
8×10^{-4}	894.82	28.17	35.97	0.0026	94.82	2493.2	0.948	1.2
1×10^{-3}	889.22	26.11	25.59	0.0023	95.43	2407.2	0.954	1.1
1.2×10^{-3}	890.97	27.07	23.28	0.0020	95.98	2655.9	0.960	0.90
2.0×10^{-3}	877.69	29.39	19.55	0.0018	96.44	2811.5	0.964	0.80

Generally if displacement of E_{corr} is >85 mv, towards anode or cathode with respect to E_{corr} of uninhibited solution, then the inhibitor is categorized as either cathodic or anodic type [43].

In our study, the maximum displacement of E_{corr} were 51 and 27 mV for NaCl and HCl solutions respectively. This result indicates that Salen acts as a mixed type inhibitor.

As can be seen from tables 1 and 2, β_c and β_a values were changed with an increase in Salen concentration. This means that the presence of Salen in the solutions does not change the processing mechanism. The analysis of the values given in these tables clearly shows that inhibition efficiency increases with the concentration reaching the maximum value of 96.44% for NaCl 3.5% and 95.02% for HCl 1 M at ($2X10^{-2}$M).

Adsorption isotherm considerations

It is well known that the adsorption of the inhibitors at the metal/solution interface is the initial step in the inhibition mechanism. Organic inhibitors exhibit inhibition ability via adsorption on the metal interface and forming a protective film. Indeed, the adsorption of an organic molecule occurs because the interaction energy between an inhibitor and a metallic surface is higher than water molecules and metallic surface [44,45].

It causes that the number of active sites necessary for the corrosion reaction is reduced. The adsorption isotherm can provide the basic information about the interaction between the inhibitor and the metal surface [46,47]. In this study attempts were made to fitthe θ values to different isotherms including Langmuir, Temkin and Freundlich.

The values of linear regression coefficients confirmed the adsorption of Salen in both 3.5 % NaCl and 1M HCl solutions following the Langmuir adsorption isotherms (figures 3, 4). In This case, the surface coverage (θ) of the inhibitor on the steel surface is related to the concentration of inhibitor in the solution according to the following equation [48]:

$$\frac{C_{inh}}{\theta} = \frac{1}{K_{ads}} + C_{inh} \qquad (7)$$

where C_{inh} is the concentration of the inhibitor, K_{ads} is the adsorption constant obtained from the intercept of the straight line.

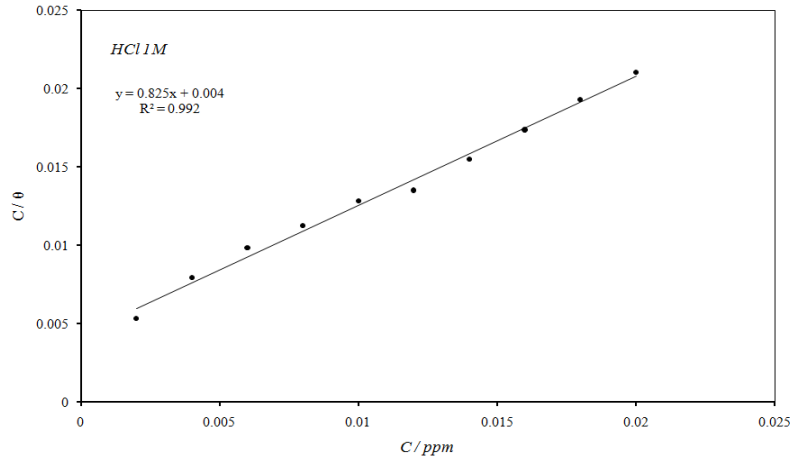

Figure 3. Langmuir adsorption plots for carbon steel in 1 M HCl containing various concentrations of the Salen at 25°C

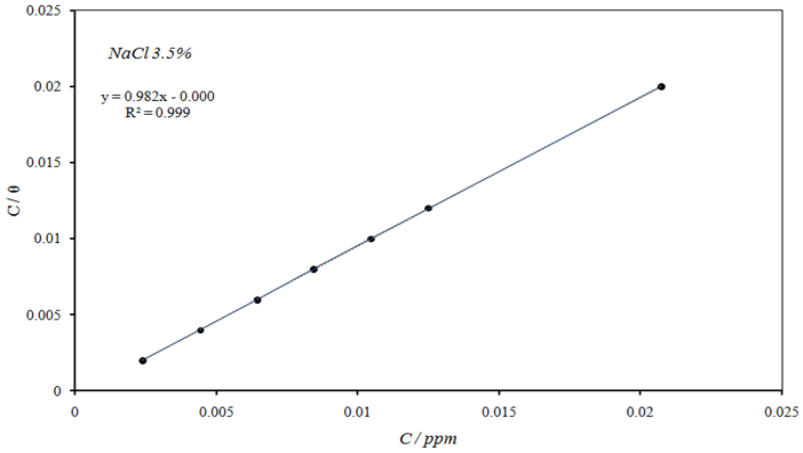

Figure 4. Langmuir adsorption plots for carbon steel in 3.5% NaCl containing various concentrations of the Salen at 25°C

This kind of isotherm involves the single layer adsorption [49,50]. The values of K_{ads} calculated from the intercept of the isotherm lines were 8.22 and 8.32 for carbon steel in HCl 1M and NaCl 3.5 % repectively. Generally, K_{ads} shows the strength of the adsorption forces between adsorbate and adsorbent. The high values of K_{ads} reflects the high adsorption capacity of inhibitor and so better inhibition efficiency [51].

Quantum chemical calculations

Here quantum chemical calculation was used to find out a relationship between inhibitors and their corresponding inhibition efficiency. Some quantum chemical parameters, which influence the electronic interaction between surface atoms and inhibitor, are the HOMO and LUMO energies, the energy gap EHOMO- ELUMO (ΔE), dipole moment (μ) elctronegativity (χ) and global hardness (η). The frontier orbitals (HOMO, LUMO) of Salen are plotted in Figure 5.

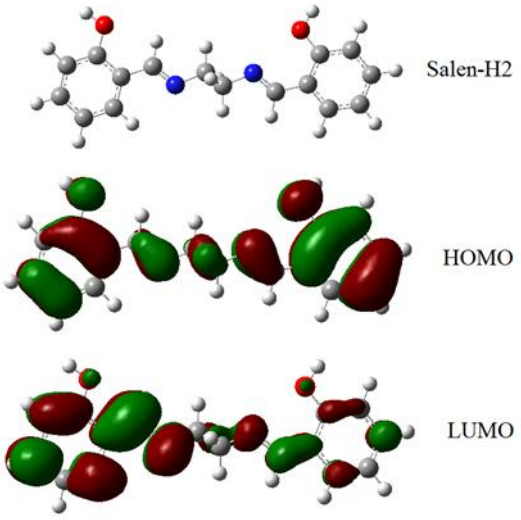

Figure 5. Spin density isosurface for HOMO and LUMO orbital's of Salen

The spatial distribution of HOMO and LUMO and their energy gap reflect that the chemical stability is important since HOMO and LUMO mediate the hole and electron transfers respectively. The HOMO represents the ability to donate electrons to unoccupied d orbital of the metal atom. Therefore, higher value of E_{HOMO} facilitates adsorption by influencing the transport process through the adsorbed layer. As an electron acceptor, LUMO represents the ability to obtain electrons from metal atom to form feedback bonds. Thus, a low value of E_{LUMO} indicates that the inhibition efficiency of that inhibitor is higher. Moreover, the gap between HOMO–LUMO energy levels of

molecules was another important parameter. In the same way, lower value of ΔE of an inhibitor causes higher inhibition efficiency [52,53].

Ionization potential and electron affinity values are hereby used to get the elctronegativity (χ) and global hardness (η) of the molecule. These two factors can be approximated by the energy of the frontier HOMO (H) and LUMO (L) molecular orbitals using the Koopmans' theorem $(IP \cong -\epsilon_H \; and \; EA \cong -\epsilon_L)$ [54].

$$\chi = {}^{1}/_{2}\,(IP + EA) \; and \; \eta = {}^{1}/_{2}\,(IP - EA) \qquad (8)$$

It has been reported in literature that lower value of hardness and higher value of electronegativity enhance inhibition efficiency [55]. Also, the computational study which has revealed the dipole moment (μ) is well related to the inhibition efficiency. In fact, the inhibition efficiency of molecules can be improved with increasing the dipole moment.

Also, ∆ N shows inhibition effect resulted from electron donation from inhibitors to metal surface and can be calculated by [56]:

$$\Delta N = (\chi_{Fe} - \chi_{inh})/[2(\eta_{Fe} + \eta_{inh})] \qquad (9)$$

where χ_{Fe} and χ_{inh} are the absolute electronegativity of steel and inhibitor respectively and η_{Fe} and η_{inh} are the absolute hardness of steel and the inhibitor respectively. According to Pearson's electronegativity scale and using a theoretical value of 7 eV/mol and 0 eV/mol for χ_{Fe} and η_{Fe} respectively, ΔN was calculated. According to literature, if the value of ΔN< 3.6, the inhibition efficiency of molecules can be improved by increasing the electron-donating ability to the metal surface [57].

Calculations were performed with DFT /B3LYP method using 6-31+G (d,p) basisset. Quantum chemical parameters, such as HOMO and LUMO energies, energy gap (ΔE), dipolemoment (μ), ionization potentioal (IP), electronaffinity (EA), elctronegativity (χ), global hardness (η) and the fraction of electrons (ΔN) transfer from inhibitors to metal surface are tabulated in Table 3.

Table 3. The calculated quantum chemical descriptors for Salen

Compound	E_{HOMO} (eV)	E_{LUMO} (eV)	ΔE (eV)	IP (eV)	EA (eV)	χ (eV)	η (eV)	ΔN (eV)
Salen H2	-5.03	-1.74	3.29	5.03	1.74	4.16	1.64	1.1

Therefore, based on all data in table 3, Salen can be considered as a good corrosión inhibitor.

Computational Dynamics Simulation

Adsorption behavior of inhibitor compounds can be very important to determine their corrosion behavior on metal surface. In this study, MD simulations were carried out to analyze the particular adsorption behavior of Salen on Fe (0 0 1) surface.

The calculated interaction energy obtained from molecular dynamics simulation were 9.577×10^{5} kcal.mol^{-1}. Moreover, the value of $E_{intereaction}$ suggests stability of adsorptive system. More negative value of $E_{intereaction}$ suggests a more stable adsorption system and leads to the higher inhibitory action.

Mechanism of Inhibition

The adsorbtion of Salen on the carbon steel surface can be explained by displacing water molecules from the carbon steel surface via the sharing of lone pair of electrons between the N and /or O atoms and iron. Besides, other possible interactions are donor–acceptor interactions between the π-electrons and vacant d-orbitals of iron.

Conclusions

Salen was investigated for its corrosion inhibition potential on the carbon steel in 3.5% NaCl and 1M HCl solutions using potentiodynamic polarization curves, quantum chemical calculation, and molecular dynamics (MD) simulation methods. It can be concluded that this compound is a good inhibitor for carbon steel (A105). The values of associated electrochemical parameters in various concentrations of Salen solutions are determined by extrapolation of anodic and cathodic Tafel lines. A maximum of inhibition efficiency 96.44% for NaCl 3.5% and 95.02% for HCl 1 M could be achieved with this inhibitor by electrochemical potentiodynamic investigation.

Maximum displacement of E_{corr} were < 85 mV which showed that Salen acted as mixed type inhibitors. Quantum chemical calculations and MD simulation also supplemented the results of electrochemical technique and showed that the corrosion inhibition performances of Salen could be related to their E_{HOMO}, E_{LUMO}, and dipole moment (μ) values.

Acknowledgement

We are thankful to the Payame Noor and Islamic Azad University Lamerd Branch for their support and encouragements.

References

[1]. Roberge P.R. *Handbook of Corrosion Engineering;* Mc Graw-Hill Professional Publishing: New York, **1999**.

[2]. Khamis M.M., Saleh M., Awad I., El-Anadouli B.E. *Corros. Sci.,* 2013, **74**:83

[3]. Park J.K., Jeong N.H. *Iran. J. Chem. Chem. Eng*., 2016, **35**:85

[4]. Abdallah M., Asghar B.H., Zaafarany I., Fouda A.S. *Int. J. Electrochem. Sci*. 2012, **7**:282

[5]. Jing-Mao Z., Li J., *Acta Phys. Chim. Sin*., 2012, **28**:623

[6]. Mehdaoui R., Khelifa A., Khadraoui A., Aaboubi O., Hadj Ziane A., Bentiss F., Zarrouk A., *Res. Chem. Intermed.,* 2016, **42**:5509

[7]. Eguchi K., Ishiguro Y., Ota H. *Corrosion*, 2015, **71**:1398

[8]. Saviour A.U. *J. Mol. Liq*., 2016, **219**:946

[9]. Muthukrishnan P., Jeyaprabha B., Tharmaraj P., Prakash P. *Res.Chem. Intermed*., 2015, **41**:5961

[10]. Ramya K., Anupama K.K., Shainy K.M., Abraham J. *J. Taiwan Inst. Chem. Eng*., 2016, **58**:517

[11]. Ya G.A., *Prot. Met. Phys. Chem*., 2015, **51**:1140

[12]. Yadav M., Sinha R.R., Kumar S., Bahadur I., Ebenso E.E. *J. Mol. Liq*., 2015, **208**:322

[13]. Li X., Xie X., Deng S., Du G. *Corros. Sci*., 2015, **92**:136

[14]. Farag A.A., Tamer A.A. *J. Ind. Eng. Chem*., 2015, **21**:627

[15]. Khaled K.F. *Corros. Sci*., 2010, **52**:3225

[16]. Deyab M.A. *Electrochim. Acta*, 2016, **202**;262

[17]. Farag A.A., Hegazy M.A. *Corros. Sci*., 2013, **74**:168

[18]. Ren X., Xu S., Chen S., Chen N., Zhang S. *RSC Adv*., 2015, **5**:10169

[19]. Bozorg B., Shahrabi Farahani T., Neshati J., Mohammadi Ziarani G., Chaghazardi Z., Gholamzade P., Ektefa F. *Res. Chem. Intermed*., 2015, **41**;6057

[20]. Khaled K.F. *Electrochim. Acta*, 2010, **55**:6523

[21]. Zarrok H., Zarrouk A., Salghi R., Elmahi B., Hammouti B., Al-Deyab S.S., Ebn Touhami M. *Int. J. Electrochem. Sci*., 2013, **8**:11474

[22]. John S., Joseph A. *Indian J. Chem. Technol*. 2012, **19**:195

[23]. Adardour K., Touir R., Elbakri M., Ramli Y., Ebn Touhami M., El Kafsaoui H., Mubengayi C.K., Essassi E.M. *Res.Chem. Intermed*., 2013, **39**:4175

[24]. Chidiebere M.A., Ogukwe C.E., Oguzie K.L., Eneh C.N., Oguzie E.E. *Ind. Eng. Chem. Res*., 2012, **51**;668

[25]. Bentiss F., Lebrini M., Lagrenee M., Traisnel M., Elfarouk A., Vezin H. *Electrochim. Acta*. 2007, **52**:6865

[26]. Lebrini M., Traisnel M., Lagrenee M., Mernari B., Bentiss F. *Corros. Sci*., 2008, **50**:473

[27]. Yadav M.S., Kumar N., Tiwari I.B., Ebenso E.E. *J. Mol. Liq*., 2015, **212**:151

[28]. Yadav M., Kumar S., Ranjan Sinha R., Kumar S. *J. Dispersion Sci. Technol*., 2014, **35**:1751

[29]. Debasis Behera M.Y., Sinha R.R., Yadav P.N. *Acta Metall. Sinica*, 2014, **27**:37

[30]. Yadav M., Behera D., Kumar S., Rajesh R.S. *Ind. Eng. Chem. Res*., 2013, **52**:6318

[31]. Deng S., Li X., Xie X. *Corros. Sci*., 2014, **80**:276

[32]. Arukalam I.O., Madufo I.C., Ogbobe O., Oguzie E.E. *Int. J. App. Sci. Eng. Res*., 2014, **3**:241

[33]. Signorini O., Dockal E.R., Castellano G., Oliva G. *Polyhedron*, 1995, **15**:245

[34]. *Gaussian 09, Revision B.01, Gaussian, Inc., Wallingford CT*., **2009**.

[35]. Materials Studio. Revision 6.0. San Diego, USA: Accelrys Inc., **2011**.

[36]. Oguzie E.E., Li Y., Wang S.G., Wang F. *RSC Adv*., 2011, **1**:866

[37]. Al-Mobarak N.A., Khaled K.F., Hamed M.N.H., Abdel-Azim K.M., Abdelshafi N.S. Arab. J. Chem., 2010, **3**:233

[38]. Xu B., Liu Y., Yin X.S., Yang W.Z., Chen Y.Z. *Corros. Sci*., 2013, **74**:206

[39]. Negm N.A., Ghuiba F.M., Tawfik S.M. *Corros. Sci*., 2011, **53**:3566

[40]. Warkus J., Raupach M., Gulikers G., Mater. Corros., 2006, **57**:614

[41]. Düdükcü M. Avc G. *Prog. Org. Coat*., 2016, ٢٠١٦:110

[42]. Souza F.S., Spinelli A. *Corr. Sci*., 2009, **51**:642

[43]. Poursaee A. *Cem. Concr. Res*., 2010, **40**:1451

[44]. Bockris J.O., Swinkels D.A.J. *J. Electrochem. Soc*., 1964, **111**:736743

[45]. Saleh M.M., Atia A.A. *J. Appl. Electrochem*., 2006, **36**:899

[46]. Kumar S., Sharma D., Yadav P., Yadav M. *Ind. Eng. Chem. Res*., 2013, **521**:4019

[47]. Musa A.Y., Kadhum A.A.H., Mohamad A.B., Takriff M.S. *Corros. Sci*., 2010, **52**:3331

[48]. Herrag L., Hammouti B., Elkadiri S., Aouniti A., Jama C., Vezin H., Bentiss F. *Corros. Sci*., 2010, **52**:3042

[49]. Outirite M., Lagrenée M., Lebrini M., Traisnel M., Jama C., Vezin H. *Electrochim. Acta*, 2010, **55**:1670

[50]. Elayyachy M., El Idrissi A., Hammouti B. *Corros. Sci*., 2006, **48**:2470

[51]. Refaey S.A.M., Taha F., Abd El-Malak A.M. *App. Sur. Sci*., 2004, **236**:175

[52]. Sagdinc S.G., Kara Y.S. *Prot. Met. Phys. Chem*., 2014, **50**:111

[53]. Mistry B.M., Patel N.S., Sahoo S., Jauhari S. *Bull. Mater. Sci*., 2012, **35**:459

[54]. Pearson R.G. *Inorg. Chem*., 1988, **27**:734

[55]. Amin M.A., Khaled K.F., Mohsen Q., Arida H.A. *Corros. Sci*., 2010, **52**:1684

[56]. Pearson R.G. *J. Am. Chem. Soc*., 1963, **85**:3533

[57]. Lukovits I., Kalman E., Zucchi F. *Corrosion*., 2001, **57**:3

How to cite this manuscript: Homa Shafiekhani, Fatemeh Mostaghni*, Kolsoum Ejraei. Electrochemical and Simulation Analysis of Salen as a Corrosion Inhibitor. Chemical Methodologies ٢(2), 201٨, 1١٤-1٢٧. DOI: 10.22631/chemm.2018.112578.1030.